ORNL/SPR-2018/866
Revision 1

Fabrication and microstructural analysis of ceramic fuel derived from sol-gel and powder routes

Nuclear Technology Research and Development

Prepared for
U.S. Department of Energy
Advanced Fuels Campaign
S.C. Finkeldei
J. Kiggans
R. Hunt
K.A. Terrani
A.T. Nelson
Oak Ridge National Laboratory
May 2018
M3NT-18OR020201052

SUMMARY

Within the Advanced Fuels Campaign the Oak Ridge National Laboratory is looking into the fabrication of enhanced UO_2 fuel candidates. Early in FY 18 an open-port glove box line was set up enabling the fabrication and initial characterization of potentially enhanced fuel candidates. The fabrication processes available at the Oak Ridge National Laboratory are unique owing to its UO_3 microsphere feedstock compared to commonly used powder feedstocks. The reported activities demonstrate the feasibility of fabricating advanced UO_2-Molybdenum ceramics with an enhanced thermal conductivity and high densities. Further development of the fabrication routes and a variety of different dopants is expected to result in a matrix of different advanced fuel candidates. Following initial property screening, the in-reactor performance and suitability of these fuel candidates will be probed in the MiniFuel irradiation set-up at the Oak Ridge National Laboratory.

INTENTIONALLY BLANK

CONTENTS

FIGURES

TABLES

ACRONYMS

AFC	Advanced Fuels Campaign
ATF	accident tolerant fuel
EDS	energy dispersive x-ray spectroscopy
LFA	laser flash analysis
ORNL	Oak Ridge National Laboratory
PCI	pellet-cladding interaction
rpm	revolutions per minute
SEM	scanning electron microscopy
TD	theoretical density
XRD	x-ray diffraction

ACKNOWLEDGMENTS

This work was supported by the US Department of Energy Office of Nuclear Energy (DOE-NE) Advanced Fuels Campaign (AFC).

FABRICATION AND MICROSTRUCTURAL ANALYSIS OF CERAMIC FUEL DERIVED FROM SOL-GEL AND POWDER ROUTES

1. INTRODUCTION

The Advanced Fuels Campaign (AFC) is seeking accident tolerant fuels (ATF) with superior properties compared to UO_2. Considering that UO_2 is still the most commonly used fuel in nuclear power plants for energy production, this work focuses on the development and characterization of enhanced UO_2 based fuels with additives. Key aspects for the design of enhanced UO_2 fuel candidates are engineering of the fuel microstructure. This is conventionally approached through either addition of dopants or larger quantities of secondary inert phases. Dopants consist of secondary cations introduced through either wet or dry additions to the UO_2 feedstock during processing steps. They are added at hundred- to thousand-weight parts per million levels. This is typically either below or slightly above the solubility of the transition metal in the UO_2 lattice. This causes the secondary cations to either reside on uranium sites or precipitate out as secondary phases at very small volume fractions. The goal of this approach is to either grow grain sizes and/or alter the mechanical properties of UO_2 of nominal purity. Larger grains have the effect of extending the time it takes for fission products to reach a grain boundary, where they have a quicker escape route. Therefore, fuel with enlarged grains will lead to a slower fission gas release. The addition of Cr_2O_3 has been found to achieve this goal and in parallel lower the fracture strength of UO_2. This exasperates cracking of the fuel pellet, limiting its' ability to exert force on the cladding, and thereby reducing pellet-cladding interaction (PCI).

The second approach is to incorporate larger volume fractions of a secondary phase. The goal of this approach has generally been to use high thermal conductivity phases to increase the thermal conductivity of the fuel pellet during service. The lower fuel temperatures and thermal gradients resulting from this approach increases the margin to melt as well as stored power in the core. Lower temperatures also limit fission product mobility and may reduce release during normal operation. The challenge of adding an inert, non-uranium bearing phase comes in the loss of U-235 that occurs unless enrichment is increased.

In the present work, molybdenum was chosen as an inert secondary phase. Molybdenum was chosen due to its enhanced thermal conductivity and moderate thermal neutron absorption cross-section [1]. In contrast to most approaches presented in the open literature [1-3], the efforts at the Oak Ridge National Laboratory (ORNL) were started from a sol-gel derived precursor. Results will be compared to reference ceramics starting from a conventional powder precursor. Once these potentially advanced fuel candidates are fabricated and thoroughly characterized, irradiation will take place in the MiniFuel irradiation setup at ORNL and allow for post irradiation examination to understand their response to irradiation and evaluate their suitability for in-reactor application.

2. INFRASTRUCTURE

Early in FY 18 the infrastructure for the enhanced ceramic fuel fabrication was set-up at ORNL. Five interconnected open-port glove boxes were taken into operation in the 235 laboratory and equipped for ceramic fuel fabrication and characterization (Figure 1). This facility enables infiltration, mixing and milling capabilities, cold pressing of the fuel pellets as well as high temperature sintering in diverse atmospheres. Density determinations are conveniently performed via a nitrogen pycnometer.

Figure 1: Open-port glove box line recently set-up at ORNL including mixing, milling devices and metal furnaces.

Mixing and milling processes are carried out with a SpeedMixer from FlackTek (DAC 150 FVZ-K Remote) and a high energy ball mill (SpexMill, 8000M Mixer/Miller). For calcining and debinding purposes a tube furnace from Mellen with an Inconel tube was installed (T_{max}: 1000°C, hot zone Ø 4", 7" long). Sintering is performed in a tungsten element chamber furnace from MRF. The maximum operating temperature under reducing conditions is 1900 °C and the furnace has a rather large sample chamber (Ø 4", 7" high) and is equipped with a dewpoint meter.

Supporting characterization equipment such as x-ray diffraction (XRD) currently located in different laboratories at ORNL will be moved to the 235 laboratory and the purchase of a desktop scanning electron microscope (SEM) for microstructural characterization as well as energy dispersive x-ray spectroscopy (EDS) is planned to enable a thorough on-site characterization.

3. FABRICATION OF ENHANCED UO_2 CERAMIC FUEL

The entire fabrication route of all ceramic fuel pellets was performed inside the glove boxes.

3.1 Fabrication of Mo doped pellets via milling & mixing starting from UO_3 microspheres

A UO_3 feedstock for the ceramic pellet fabrication was produced by the internal sol-gel process. A batch of UO_3 microspheres, < 75 µm, was reduced to UO_2 in Ar-4% H_2 atmosphere inside a tube furnace (Mellen) with a heating rate of 1.6 °C/min to 300 °C, 30 min dwell time and 3.2 °C/min to 600 °C, 5 hrs dwell time. The cooling rate was 5 °C/min.

The calcined spheres are the precursor for the pellet fabrication in the below described experiments.

4 g UO_2 were mixed for 30 sec with 0.1% acrawax c as a binder. Subsequent milling took place for 3 x 2 mins in a Spexmill with zirconia milling media.

UO_2 reference pellet

A reference pellet of 0.2230 g milled UO_2 was biaxially cold pressed with a 10.2 mm die at 200 MPa. A debinding step was applied in a tube furnace with an initial heating rate of 2.5 °C/min to 300 °C followed by a 30 mins dwell time, a heating rate of 5 °C/min to 630 °C with a dwell time of 1 hr and a final heating rate of 10 °C/min to 900 °C with 1 hr dwell time. The cooling step took place with 10 °C/min.

Sintering took place in Ar-4% H_2 atmosphere in a tungsten heating element furnace (MRF) at 1700 °C. Up to 300 °C a heating rate of 3 °C/min was applied, which was increased to 5 °C/min up to 200 °C with a final heating rate of 10 °C/min to 1700 °C and a sintering duration of 6 hrs. The cooling rate equaled 10 °C/min.

UO_2 pellets containing 5 vol% and 10 vol% Mo

To investigate the influence of the dopant powder size on the ceramic fuel properties two different Mo powders were used. A rather fine Mo powder from nanomaterials had a particle size <800 nm, and is referred to as fine Mo hereafter. A second more coarse Mo powder was prepared by mixing 27 g Climax Mo powder (NPA grade) and 73 g TEKMAT Mo-45 powder. This mixture is referred to as coarse Mo. 1 g acrawax c was added as binder and mixed for 10 mins in a ball mill.

UO_2 pellets with 5 vol% and 10 vol% Mo were fabricated to study the effect of the dopant concentration towards the fuel properties. The respective amounts of the calcined UO_2 spheres and the Mo powder (Table 1) were mixed for 30 secs on a Vortex mixer and milled for 3 x 2 mins in a Spexmill. The blended powders were biaxially pressed in a 10.2 mm die at 200 MPa. The debinding and sintering step were conducted at the same conditions as for the UO_2 reference pellet.

Table 1: Sample compositions fabricated from UO_2 microspheres and Mo powder.

ID	m (UO_2 & acrawax) (g)	m (Mo) (g)	vol% Mo (%)	total pellet mass (g)
21	0.2230	-	-	0.2230
23	3.8742	0.1868 (fine)	4.9	1.3465
25	3.6883	0.3851 (fine)	10.0	1.3355
27	3.8891	0.1843 (coarse)	4.8	1.3342
29	3.6974	0.3782 (coarse)	9.8	1.2964

3.2 Fabrication of Mo doped pellets via mixing starting from DUO_2 powder (AREVA)

$DUO_{2.04}$ powder from AREVA was recalcined under Ar-4% H_2 atmosphere. Previous calcination conditions were applied. Here, 0.484 g fine Mo powder were mixed with 0.005 g acrawax c for 1 min. The UO_2 and Mo powders were mixed in a FlackTek mixer for 30 sec at 650 rpm in the amounts given in Table 2.

Due to the different feedstock, the pressing force for these pellets was lowered to 40 MPa and kept for 2 mins to obtain intact pellets. A reference pellet without Mo was pressed at the same conditions.

The same debinding and sintering conditions as mentioned above were applied.

Table 2: Amounts of UO_2 and Mo powder for pellet fabrication from a UO_2 powder feedstock.

ID	M (UO_2 & acrawax) (g)	m (Mo) (g)	vol% Mo (%)	total pellet mass (g)
77	0.4233	-	-	
78	0.4206	0.0478	10.8	0.4206

3.3 Developing a fabrication process for microsphere coating

To avoid a milling step of the calcined spheres, within this synthesis approach the spheres were directly mixed and subsequently pressed into pellets. No binder was added for these fabrication routes. The different ratios and sphere size selections for pellets 46, 48 and 49 are given in Table 3 and were chosen by taking findings from the literature [4] into account. The calcined UO_2 spheres were mixed for 10 sec on a Vortex at low speed. After loading a 4 mm die the die was vibrated for 20 sec to allow for dense packing of the spheres. For pellet 49 the die was subsequently loaded starting from the biggest spheres to the smallest spheres with vibrating steps in between each sphere loading step.

A second approach to obtain highly dense UO_2 pellets followed Ayer and Soppet [5] who determined a model to calculate packing efficiencies for ternary size systems of spherical shape in a 1:1:1 ratio (pellet 47).

All pellets were biaxially cold pressed for 2 mins with 200 MPa. The pellets were sintered at the same conditions as mentioned above.

Table 3: Composition of UO_2 pellets directly fabricated from microspheres with the corresponding sphere size of the dried UO_3 spheres.

ID	ratio	mass (g) <75 µm	mass (g) 150-212 µm	mass (g) 212-300 µm	mass (g) 300-425 µm
46	3:7	0.0398	-	-	0.0833
47	1:1:1	0.0412	-	0.039	0.0397
48	67:23:10	0.0147	0.0265	-	0.0792
49	67:23:10	0.0118	0.0265	-	0.0792

4. STRUCTURAL, MICROSTRUCTURAL AND THERMAL PROPERTIES OF THE FUEL CERAMICS

To unravel the influence of the fabrication route, dopant size as well as concentration towards the fuel ceramic various characterization techniques were applied.

4.1 X-ray diffraction

To probe the crystal structure of the fabricated fuel candidates a UO_2 reference pellet, a pellet with 5 vol% and one with 10 vol% Mo were encapsulated in kapton foil and measured by XRD.

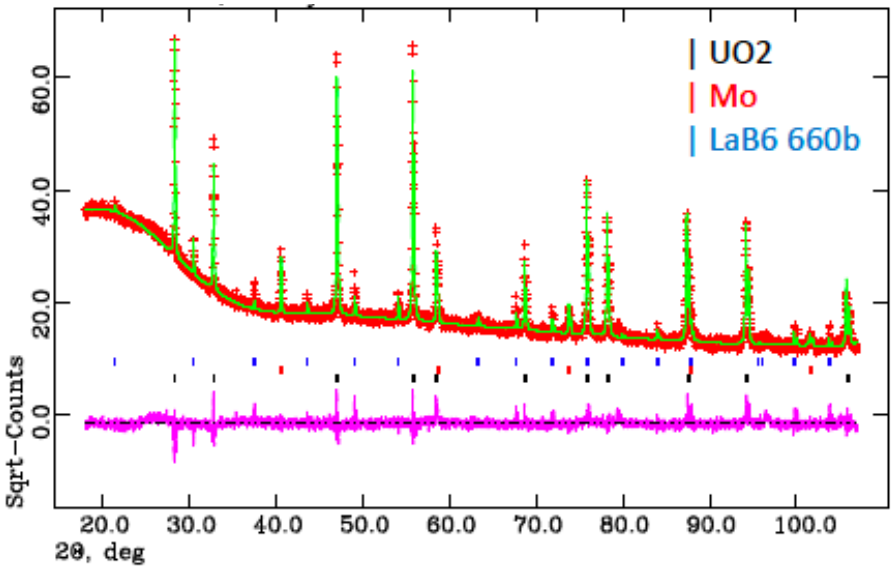

Figure 2: XRD pattern of UO_2 with 5 vol% fine Mo dopant. The pattern (red) confirm the formation of a composite ceramic with UO_2 in the cubic fluorite structure and a separate Mo phase.

LaB_6 commonly added to enable lattice parameter refinements was added as an internal standard. A cubic fluorite structure was confirmed for all samples. Moreover, the UO_2 pellets with Mo showed the presence of a second phase confirming the formation of a composite ceramic fuel as exemplarily shown for a 5 vol% Mo doped UO_2 pellet in Figure 2.

4.2 Density

The density was geometrically determined and a nitrogen pycnometer (AccuPyc II 1340, micromeritics) was set-up inside the glove box for future density measurements. The green and debinding density could only be determined for thick pellets to avoid damaging the fragile green pellets. The theoretical density of the UO_2-Mo pellets was calculated by taking into account the volume fractions of Mo (ρ = 10.28 g/cc) and UO_2 (ρ = 10.97 g/cc). UO_2 with 5 vol% Mo resulted in a theoretical density of 10.94 g/cc and UO_2 with 10 vol% Mo had a slightly lower theoretical density of 10.90 g/cc. For pure as well as Mo doped pellets fabricated by mixing and milling the green density is in the 50-60% theoretical density (TD) region and increases to the low 60% after the debinding step (Figure 3). After sintering, dense pellets with up to 96% TD were obtained. No systematic influence of the Mo dopant size or concentration was observed in the present study. For the pellets fabricated from UO_2 powder a significantly lower value of 87% and 80% TD was obtained for the pure UO_2 and UO_2 pellet containing 10 vol% Mo. Regarding the much lower pressing

pressure applied for these pellets (40 MPa) this is not surprising and a pressing and densification study will lead to an optimized density for ceramics fabricated from powder feedstock.

The UO_2 pellets directly fabricated from microspheres without any milling steps resulted in 92% - 97% TD.

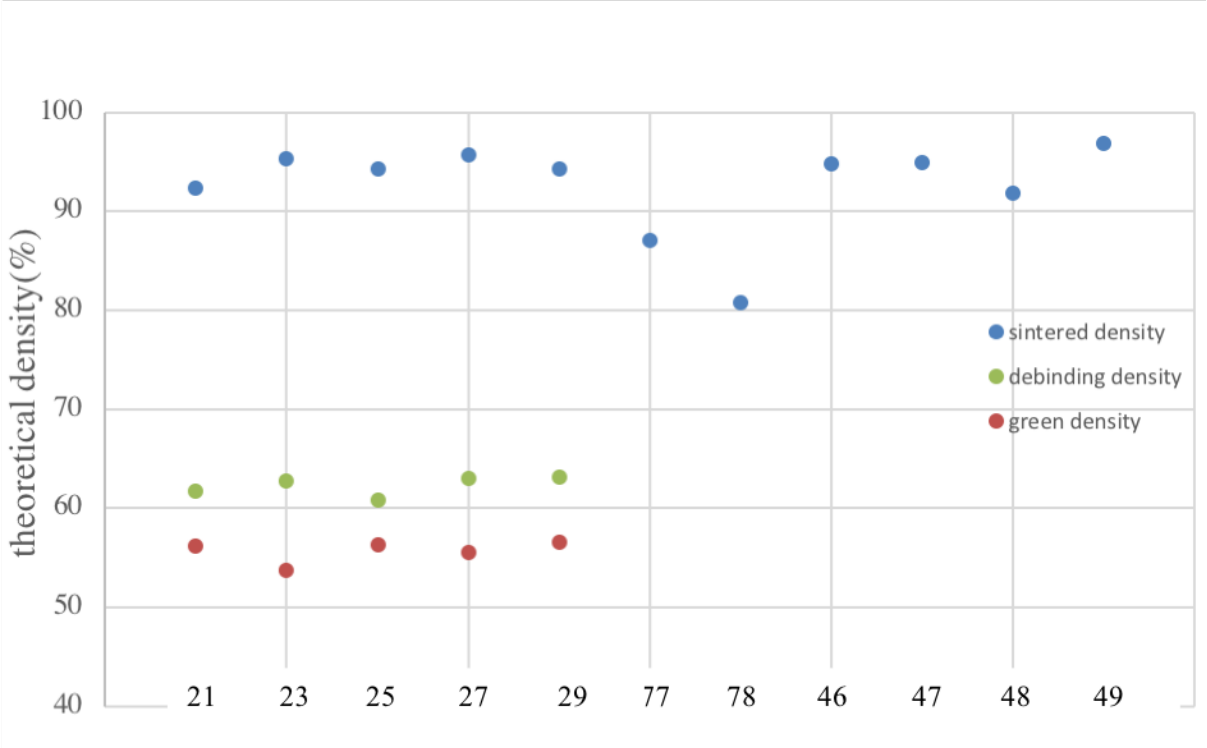

Figure 3: Green density (red), debinding density (green) and sintering density (blue) for fabricated ceramics. Samples 23 and 25 contain 5 vol% and 10 vol% fine Mo dopant, whereas 27 and 29 refer to 5 vol% and 10 vol% coarse Mo dopant. All pellet specifications can be found in Table 1, Table 2 and Table 3.

4.3 Microstructural Characterization

To gain microstructural insights all fabricated ceramics were characterized by scanning electron microscopy. EDS confirmed the formation of a composite ceramic, visible for 5 vol% Mo doped UO_2 ceramics for fine (Figure 4a) and coarse (Figure 4c) Mo starting powders. Further analysis is needed to better characterize the morphology of the Mo relative to the UO_2 grains.

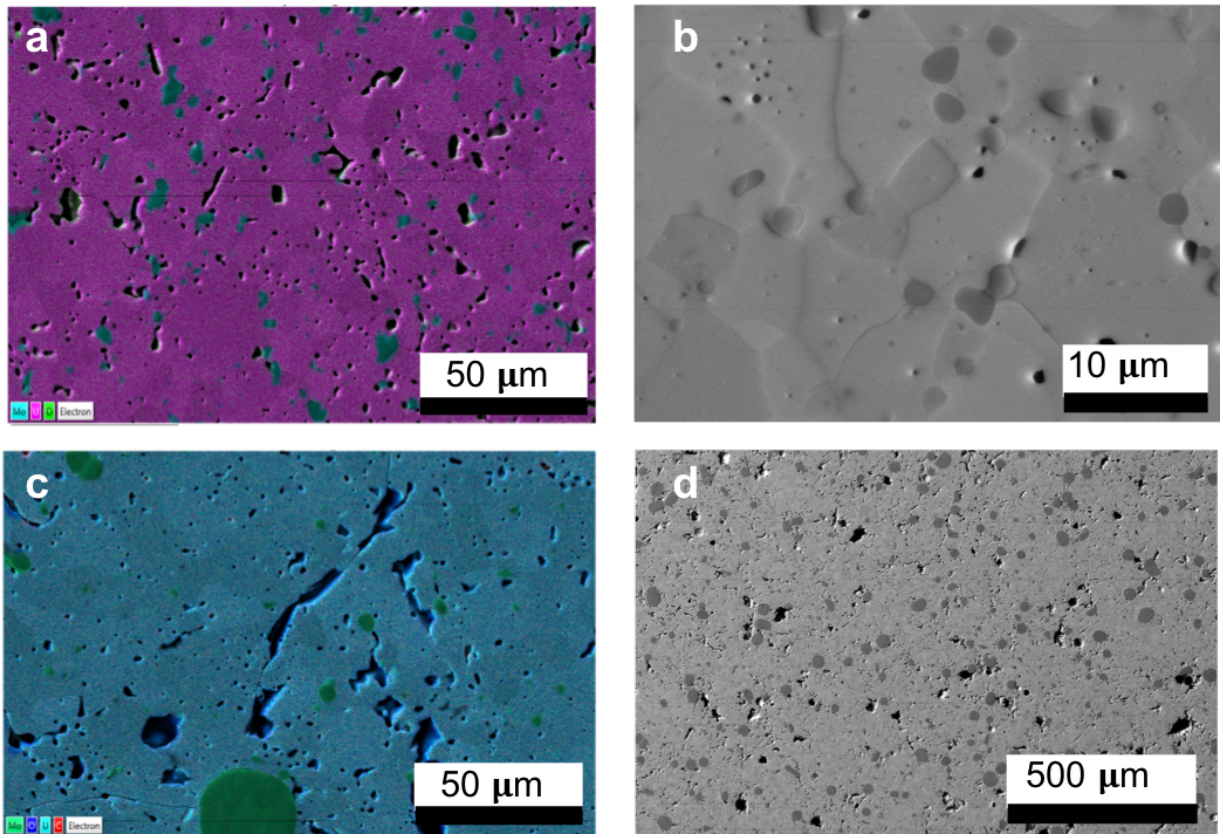

Figure 4: EDX mappings and BSE images of 5 vol% Mo doped UO_2 ceramics with fine Mo (a&b) and coarse Mo (c&d).

The pellets directly pressed from the microsphere mixtures showed fairly dense microstructures. For some pellets (ID 47 and 49) a blackberry structure was observed at the pellet surface (
Figure 5b and e). However, polishing and subsequent imaging at the cross section attributed the black berry structure as surface feature and a rather dense microstructure throughout the pellet. SEM images of the blackberry structure revealed a polycrystalline structure of the microspheres. The pellets exhibit heterogeneous grain sizes with large grains in the range of > 100 µm as well as <10 µm grains.

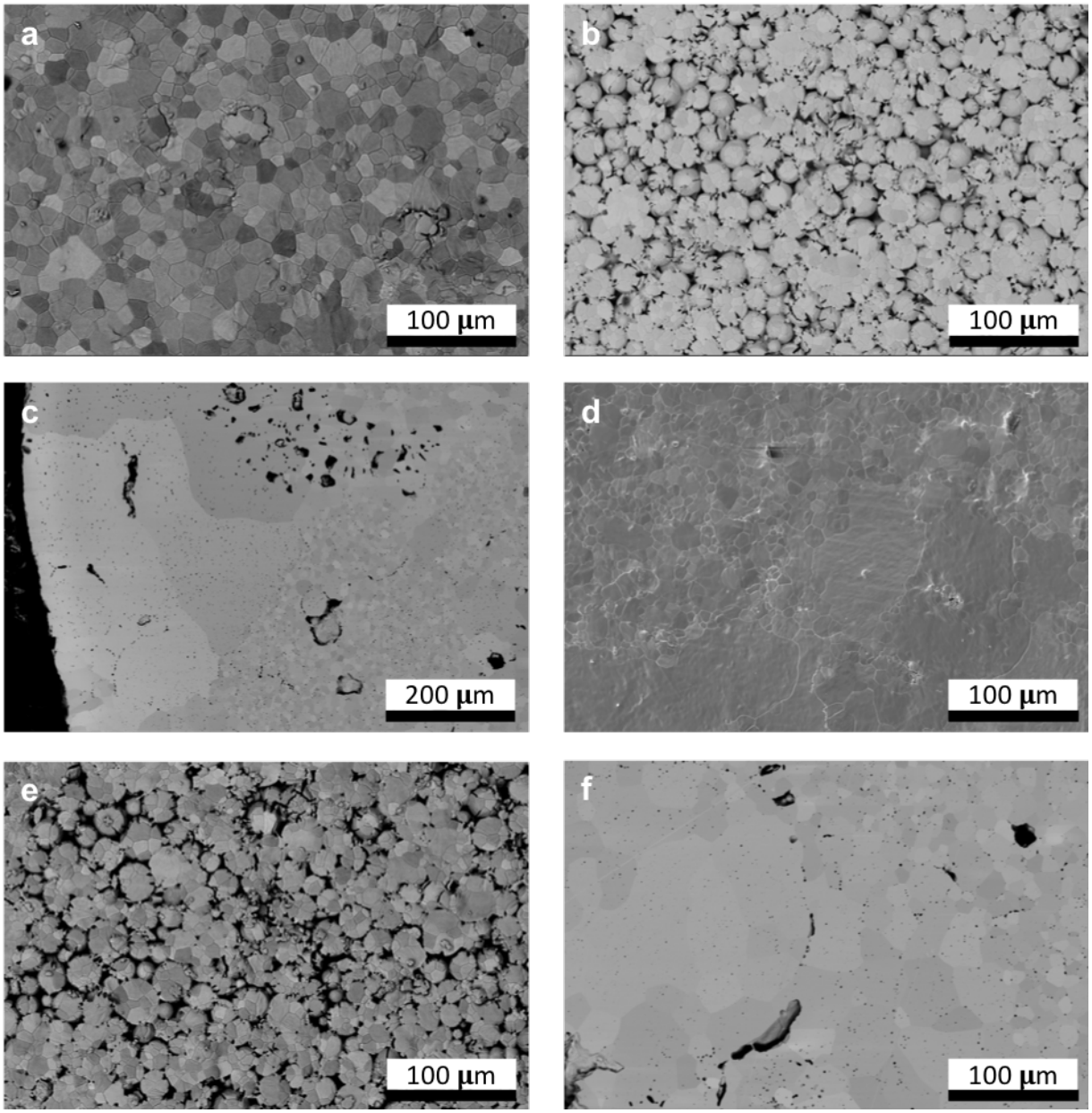

Figure 5: SEM images of UO_2 directly fabricated from sol-gel microspheres, (a) fabricated from two different sized microspheres, (b&c) 1:1:1 mixture of three different microsphere sizes at the surface (b) and at the cross section after polishing (c), (d-f) fabricated from three different sizes for direct mixing of all three sizes (d) and subsequent mixing from the biggest to the smallest size (e-f) at the surface (e) and at the pellet cross section after polishing (f).

4.4 Thermal Conductivity

In order to derive the thermal conductivity, the thermal diffusivity was measured (Netzsch, LFA457 in Ar-4% H_2) for a pure UO_2 pellet as well as for the 5 vol% and 10 vol% fine and coarse Mo-UO_2 pellets. The temperature dependent diffusivity data are plotted in Figure 6.

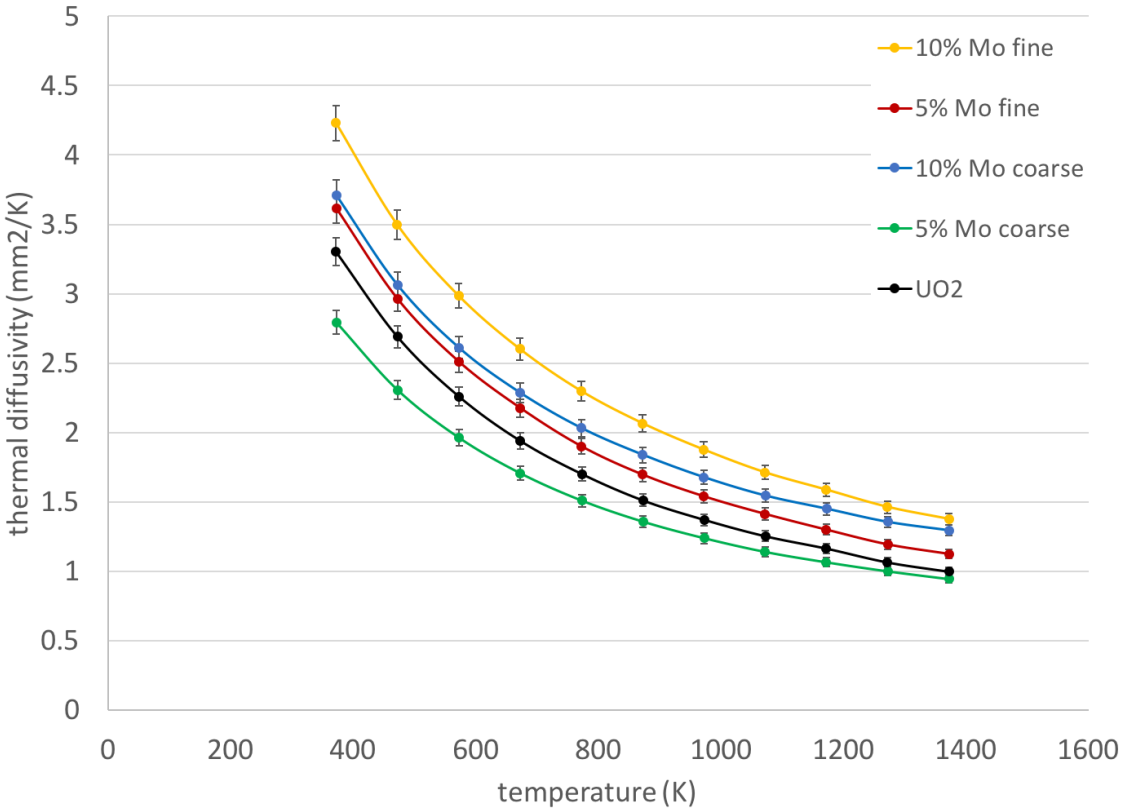

Figure 6: Thermal diffusivity data measured by laser flash analysis (LFA) for a UO_2 reference pellet (black), fine 5 vol% (red) and 10 vol% (yellow) and coarse 5 vol% (green) and 10 vol% (blue) Mo doped pellets. According to the ASTM standard [6] the thermal diffusivity data determined by LFA have a standard error of 3%.

The thermal conductivity k was calculated via:

$$k = \alpha \cdot \rho \cdot c_p \quad (1)$$

with the thermal diffusivity α, the density ρ and the heat capacity c_p. The density was measured geometrically for each sample at room temperature. The density changes due to thermal expansion were assumed to be dominated by UO_2, because UO_2 has a larger thermal expansion coefficient than Mo and second UO_2 is being the main phase of the fuel pellet. Thermal expansion values for UO_2 were taken from Conway [7] who reports them for a 95.5% TD pellet and applied to correct for the measured density at elevated temperatures. The specific heat for UO_2 and Mo were taken from Moore [8] and Lehman [9]. Heat capacities for the UO_2-Mo samples were calculated by taking the mass fraction ß = 0.046 (5 vol% Mo) and ß = 0.095 (10 vol% Mo) for the literature data into account. Figure 7 depicts the thermal conductivity for the fabricated samples and reference data for UO_2 [10, 11]. The thermal conductivity of molybdenum is much higher in comparison to UO_2 and follows a linear trend between 139 W/m·K at 373 K [12] and

99.7 W/m·K at 1300 K [13]. Literature data from Fink [10] corresponding to a 95% TD UO_2 sample and from White for $UO_{2.000}$ [11] are plotted for comparison with the here derived data in Figure 7 (grey curves).

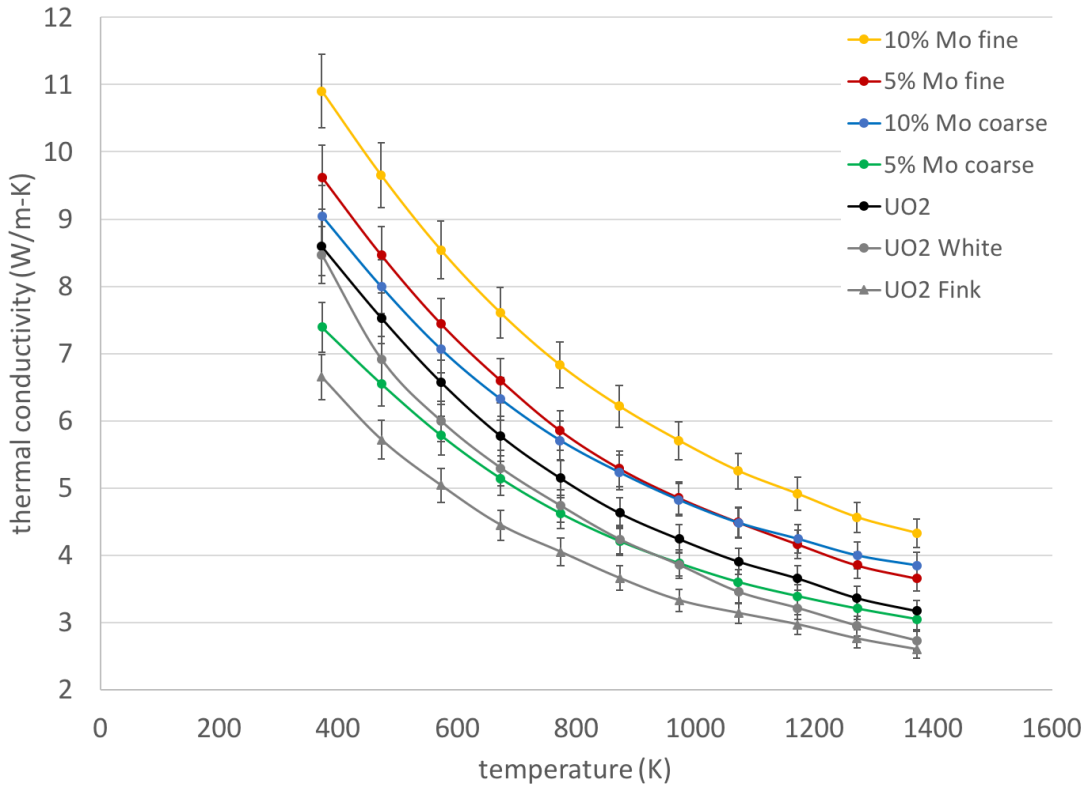

Figure 7: Temperature dependent thermal conductivity curves for a UO_2 reference pellet (black), fine 5 vol% (red) and 10 vol% (yellow) and coarse 5 vol% (green) and 10 vol% (blue) Mo doped pellets. For comparison literature data for a 95% TD UO_2 sample (grey) are plotted, which were derived from the review paper by Fink [10] and from White [11]. In compliance with the ASTM Standard [6] a 3% standard error for the thermal diffusivity measurements in combination with the error of the density as well as thermal conductivity resulted in a standard error of 5% for the thermal conductivity.

The thermal conductivity for the fabricated UO_2 pellet is enhanced in comparison to the literature data. However, it becomes obvious that the literature data [10, 11] vary among each other and rather show a thermal conductivity regime for UO_2 than a single value. The addition of molybdenum led in all cases to an increased thermal conductivity, except for a 5 vol% coarse Mo doped ceramic where the thermal conductivity is lower than for the here fabricated UO_2 reference pellet. There is so far no explanation for the lower thermal conductivity of this particular specimen, and a reproducibility study is under way with a thinner, more suitable pellet for the measurement. It is likely that microstructural defects are responsible for the degraded thermal conductivity. As to be expected a higher Mo content led to a larger increase of the thermal conductivity. Besides the dopant concentration the dopant size or distribution within the UO_2 pellet seem to play an important role, with an increase of almost 40% thermal conductivity for a pellet with 10 vol% fine Mo relative to UO_2. This suggests that the morphology of the secondary phase may play an important role in the resulting thermal conductivity. Thus, for a fixed volume fraction of an inert secondary phase such as Mo, it may be possible to affect the microstructure and contiguity of the two phases to produce materials with optimized thermal conductivity, fission gas behavior, mechanical properties, or other attributes. Further studies will assess this hypothesis.

5. CONCLUSIONS & OUTLOOK

The developed fabrication routes for sol-gel derived advanced ceramic fuels show promising results: high densities and increased thermal conductivities of almost 40 % were obtained for 10 vol% Mo doped UO_2 over pure UO_2. The fabrication route starting from the microspheres without any crushing step resulted in dense pellets. Kim et al. [1] report a Mo-microcell UO_2 ceramic fabrication route starting from a powder feedstock. The thermal conductivity of these ceramics has been enhanced further in comparison to ceramics with a non-continuous dopant phase. Further development of the direct microsphere processing routes to obtain a microcell dopant structure via wet and or dry coating or infiltration procedures of the dopants seems to be a promising next step towards enhanced UO_2 fuel ceramic fabrication.

The next step is to test the irradiation response of these enhanced UO_2 fuel ceramics which will be carried out within the MiniFuel irradiation experiments. The challenge is to fabricate the pellets thin enough for the MiniFuel irradiation capsules. The as fabricated pellets currently have a thickness of 0.8 - 0.9 mm, but need to meet thickness criteria of <0.4 mm thickness. This will involve future cutting and/or polishing development of these pellets.

A thorough characterization in particular of the density is inevitable prior to irradiation tests within the MiniFuel irradiation experiments. The fuel ceramics utilized for the irradiation tests need to meet rather small diameter and thin dimension criteria to be suitable for the MiniFuel capsule design. Therefore, the nitrogen pycnometer is currently equipped with tailor-made inserts to allow for the density determination of small specimens.

6. REFERENCES

[1] D.J. Kim, Y.W. Rhee, J.H. Kim, K.S. KimJ.S. Oh, J.H. Yamg, Y.H. Koo, K.W. Song, Fabrication of micro-cell UO2-Mo pellet with enhanced thermal conductivity, J. Nucl. Mater. 462 (2015) 289-295.

[2] J.H. Yang, K.W. Song, K.S. Kim, Y.H. Jung, A fabrication technique for a UO_2 pellet consisting of UO_2 grains and a continuous W channel on the grain boundary, J. Nucl. Mater. 353 (2006) 202-208.

[3] A.R. Massih, Effects of Additives on Uranium Dioxide Fuel Behavior, Stralsaekerhets Myndigheten, 2014, 21ISSN:2000-0456.

[4] G.D. Del Cul, C.H. Mattus, A.S. Icenhour, L.K. Felker, D.F. Williams, Fuel Fabrication Development for the Surrogate Sphere-Pac Rodlet, ORNL/TM-2005/108, DE-AC05-00OR22725, 2005.

[5] J.E. Ayer, F.E. Soppet, Vibratory Compaction: I, Compaction of Spherical Shapes, J. Am. Ceram. Soc. 48 (1965) 180-183.

[6] ASTM Standard Designation: E1461, 2013 "Standard Test Method for Thermal Diffusivity by the Flash Method," ASTM International, West Conshohocken, PA, 2013.

[7] J.B. Conway, R.M. Fincel, R.A. Hein, The thermal expansion of heat capacity of UO_2 to 2200 C, Trans. Am. Nucl. Soc. 6 (1963) 153.

[8] G.E. Moore, K.K. Kelley, High-temperature heat contents of uranium, uranium oxide, and uranium trioxide, J. Am. Chem. Soc. 69 (1947) 2105-7.

[9] G.W. Lehman, Thermal properties of refractory materials, Wright Air Development Division (1960) 1-19.

[10] J.K. Fink, Thermophysical properties of uranium dioxide, J. Nucl. Mater. 279 (2000) 1-18.

[11] J.T. White, A.T. Nelson, Thermal conductivity of UO_{2+x} and U_4O_{9-y}, J. Nucl. Mater. 443 (2013) 342-350.

[12] T. Barratt, Thermal and electrical conductivities of some of the rarer metals and alloys, Proc. Phys. Soc. 26 (1913) 347-371.

[13] C. Zwikker, Physical properties of molybdenum at high temperatures, Physica 7 (1927) 71-4.